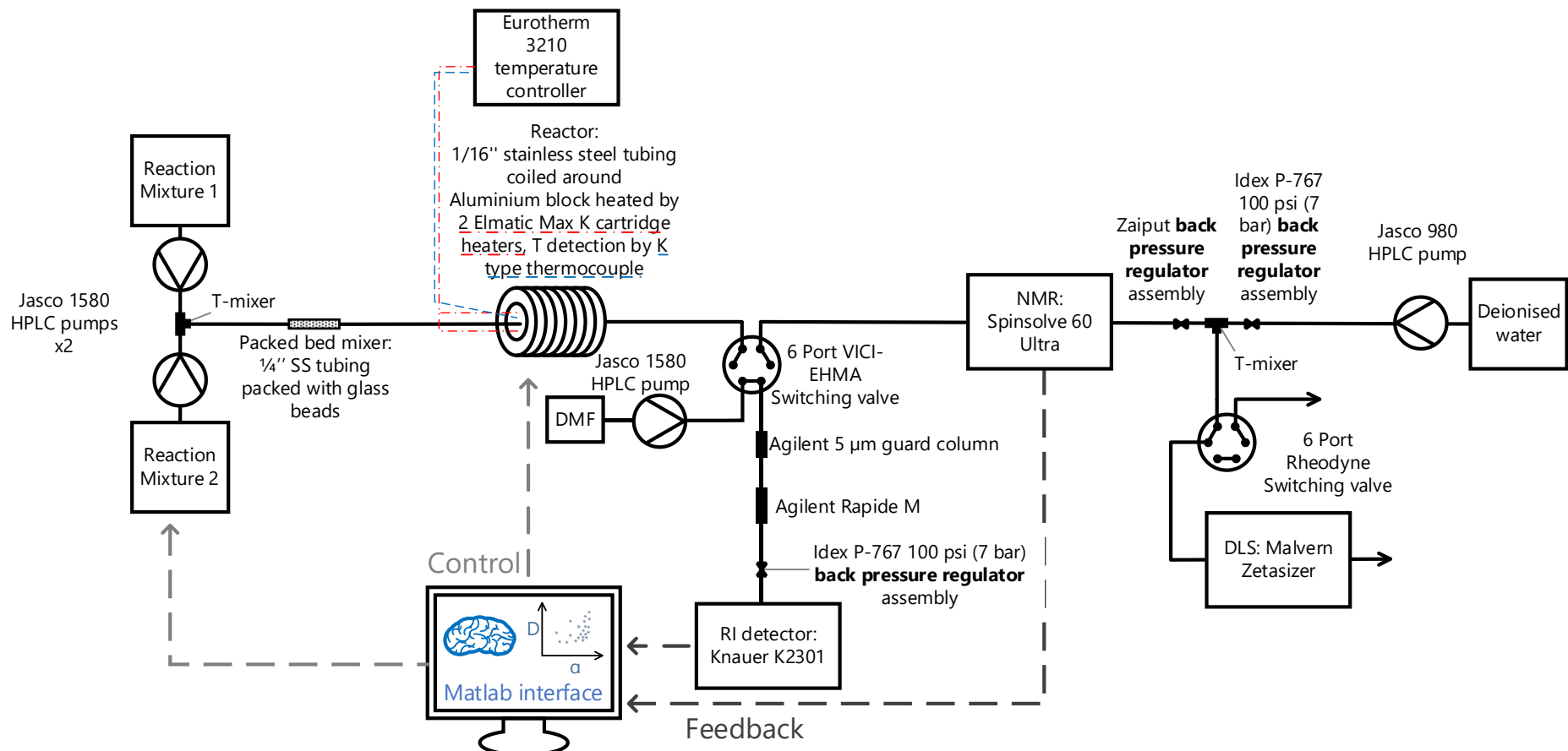


**Supporting information (SI) for:**

**Self-driving laboratory platform for many-objective self-optimisation of polymer nanoparticle synthesis with cloud-integrated machine learning and orthogonal online analytics.**

*Stephen T. Knox, Kai E. Wu, Nazrul Islam, Roisin O'Connell, Peter Pittaway, Kudakwashe Chingono, John Oyekan, George Panoutsos, Thomas W. Chamberlain, Richard A. Bourne, Nicholas J. Warren\**



**Figure S1.** Schematic for the platform used in this work.

## **Platform**

The MATLAB-controlled automated platform consisted of two Jasco PU-1580 HPLC pumps; a PFA tubular reactor (0.7 mm, I.D, 2 mL), coiled around an aluminium block heated by a Eurotherm 3210 controller fitted with two Elmatic Max K cartridges, with a Zaiput backpressure regulator (pressurised to 4 bar); a Spinsolve benchtop NMR instrument, a custom-built GPC instrument, as described in our previous work;<sup>14</sup> and a Malvern Zetasizer DLS instrument (Figure S1).

## **Online $^1\text{H}$ NMR spectroscopy**

NMR spectra were recorded using a Magritek Spinsolve 60 Ultra. They were collected using a presaturation solvent suppression routine (1s saturation pulse at 4.79 ppm of -68 dB, 7  $\mu\text{s}$  excitation pulse, spectral width of 5 kHz (32,768 points), acquisition time of 6.4 s, repetition time of 10 s and number of scans = 2) All chemical shifts are reported in ppm ( $\delta$ ).

### Online gel permeation chromatography (GPC)

The custom-built GPC setup was constructed using a Jasco PU-1580 HPLC pump (flow rate: 2 ml min<sup>-1</sup>), GPC columns (Agilent Rapide M plus guard) and a Knauer 2301 refractive index (RI) detector, all controlled by a homemade MatLab program. DMF eluent was used containing LiBr (1 % w/v). The program records the time of injection from the triggering of the switching valve, and the subsequent RI trace. Molecular weights can then be calculated from calibration to a series of near-monodisperse standards (PMMA –  $M_p$ : 885–2,200,000 g mol<sup>-1</sup>). The injection volume is approximately 3  $\mu$ l.

To improve the accuracy of the GPC data acquired, a triple injection sequence was introduced (injected at 175 s intervals). This yielded three peaks to analyse and average analytical information from. Each peak is analysed according to its injection time.

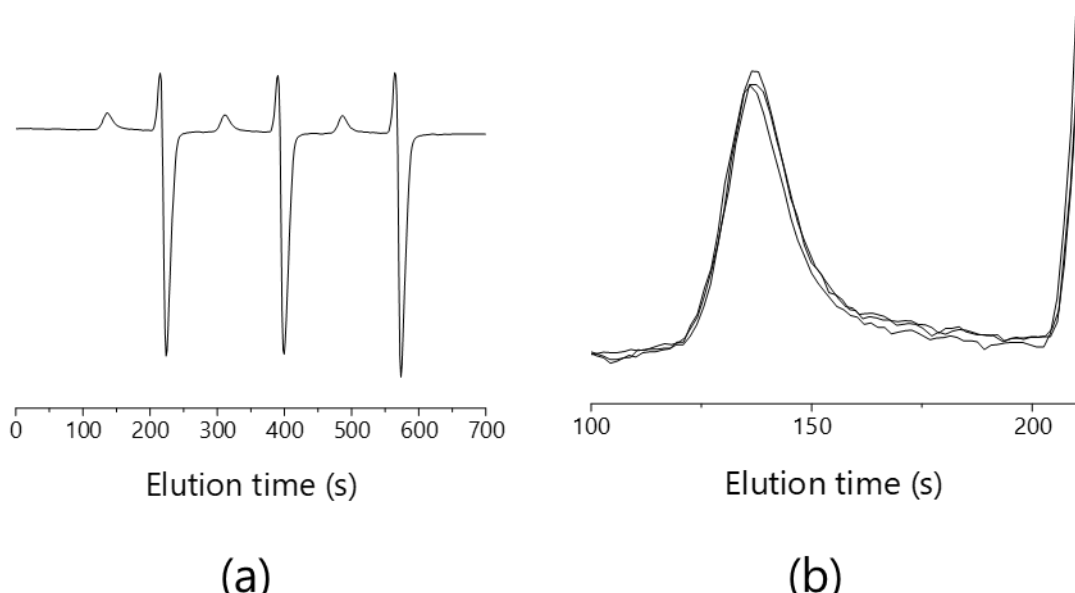


**Figure S2.** (a) Full raw chromatogram obtained from triple injection sequence from gel permeation chromatography. (b) Resultant chromatograms as calibrated to injection time.

## Online Dynamic Light Scattering

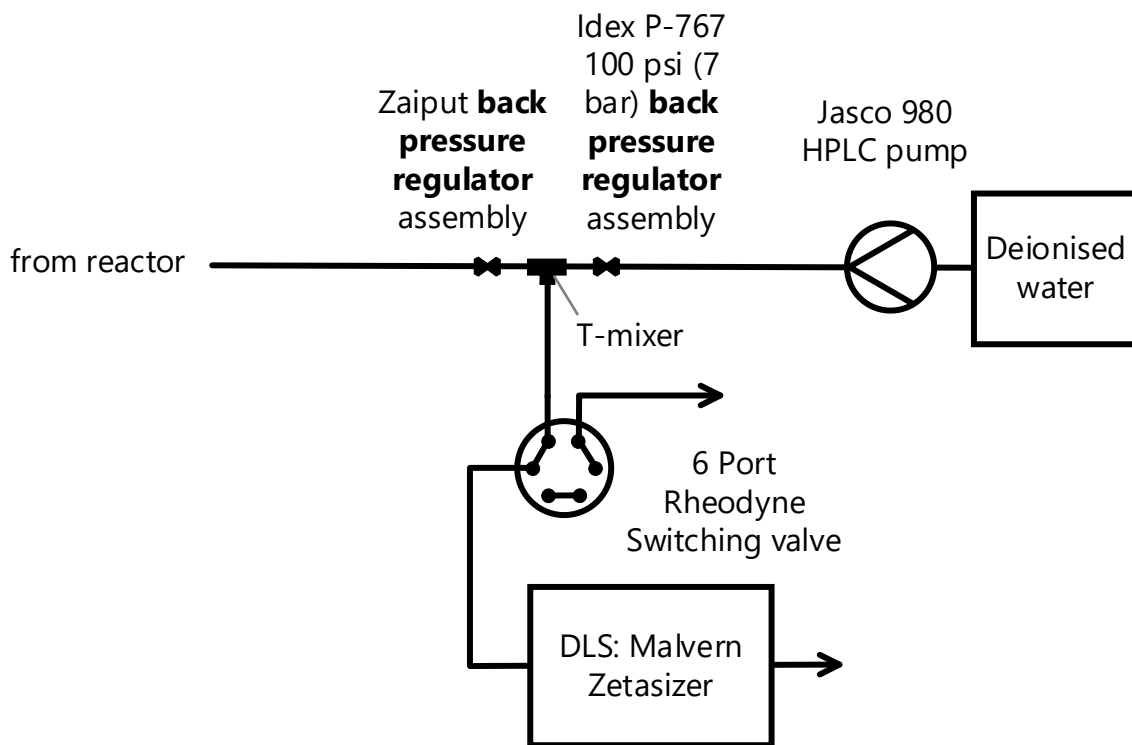


**Figure S3.** Schematic for the online dynamic light scattering analysis performed in this work

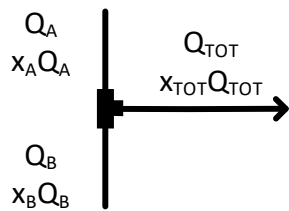
To incorporate DLS into the automated platform, a flow cell (ZEN0023 quartz cell, Hellma) was inserted into the Malvern instrument and attached to the flow stream, after a switching valve, in addition to a dilution stream to bring the product stream to the appropriate concentration for analysis. While the platform was brought to steady state, the flow was set to bypass the instrument. Upon triggering of the measurement, the dilution pump set to  $5 \text{ ml min}^{-1}$ , the total flow rate of the product stream to  $0.1 \text{ ml min}^{-1}$  and the flow redirected to pass through the flow cell, for 30 seconds, bringing the mixture to steady state.

In the absence of the ability to trigger the instrument remotely from an external program, the instrument recorded a measurement every 3 minutes and the most recent measurement acquired by the GUI. The measurement itself relied upon 5 runs of 10 seconds each, after 30s of temperature equilibration followed by the instrument's autonomous measurement optimisation. After waiting for over 2 minutes from the point of the flow being stopped, the most recent measurement was accessed by the GUI and the key information extracted for continued use.

## Mass balances and flow rate calculations

For the calculation of mass balances, we begin with the desired properties of the final product. Of that product we know the Target DP ( $DP$ ), the residence time ( $\tau$ ), the weight percent ( $w$ ), and the concentration of initiator ( $[ini]$ ), which is constant throughout. In all mass balances, a density of  $1 \text{ g cm}^{-3}$  is assumed since all reagents are in a low concentration in water.

We can construct a simple model for the mixing of two reagent streams with flowrate,  $Q$  and concentrations,  $x$  as follows:



$$Q_{TOT} = \frac{V_R}{\tau}$$

$$Q_A + Q_B = Q_{TOT}$$

$$x_A Q_A + x_B Q_B = x_{TOT} Q_{TOT}$$

$$x_A Q_A + x_B (Q_{TOT} - Q_A) = x_{TOT} Q_{TOT}$$

$$x_A Q_A + x_B Q_{TOT} - x_B Q_A = x_{TOT} Q_{TOT}$$

$$Q_A (x_A - x_B) + x_B Q_{TOT} = x_{TOT} Q_{TOT}$$

$$Q_A (x_A - x_B) = x_{TOT} Q_{TOT} - x_B Q_{TOT}$$

$$Q_A (x_A - x_B) = Q_{TOT} (x_{TOT} - x_B)$$

$$Q_A = \frac{Q_{TOT} (x_{TOT} - x_B)}{(x_A - x_B)}$$

Since all of the concentration values initially calculated as mass concentrations are scaled by the same molecular weight, then we can calculate the flow rate of pump A ( $Q_A$ ) as

$$Q_A = \frac{Q_{TOT} ([CTA] - [CTA]_B)}{[CTA]_A - [CTA]_B} \quad (1)$$

And the flow rate of pump B ( $Q_B$ ) as

$$Q_B = Q_{TOT} - Q_A \quad (2)$$

Therefore, to calculate the desired flowrates, we then need to calculate the final desired concentration of CTA ( $[CTA]$ ) in terms of the desired DP and the known chemical compositions of the two feedstock solutions.

Starting with the target DP we can calculate the mass of CTA required,

$$DP = \frac{n_{mon}}{n_{CTA}} = \frac{\frac{m_{mon} \times 1}{MW_{mon}}}{\frac{1}{m_{CTA} \times MW_{CTA}}}$$

$$\frac{m_{mon}}{m_{CTA}} = \frac{DP \times MW_{mon}}{MW_{CTA}}$$

$$m_{mon} = \frac{DP \times MW_{mon}}{MW_{CTA}} \times m_{CTA}$$

$$m_s = m_{ini} + m_{CTA} + m_{mon}$$

$$m_s - m_{ini} = m_{CTA} + m_{mon} = m_{CTA} + \frac{DP \times MW_{mon}}{MW_{CTA}} \times m_{CTA} = m_{CTA} \left( 1 + \frac{DP \times MW_{mon}}{MW_{CTA}} \right)$$

And therefore

$$m_{CTA} = \frac{m_s - m_{ini}}{\left( 1 + \frac{DP \times MW_{mon}}{MW_{CTA}} \right)}$$

If we arbitrarily assign  $m_{TOT}$  as 1;

$$w = \frac{m_s}{m_{TOT}} = m_s$$

This gives

$$m_{CTA} = \frac{w - m_{ini}}{\left( 1 + \frac{DP \times MW_{mon}}{MW_{CTA}} \right)}$$

The mass of initiator can be calculated simply from the desired concentration of initiator ( $[ini]$ ) for the experiment – in this case, 0.75 mmol dm<sup>-3</sup>. For water, the density ( $\rho$ ) can be approximated to one and again taking the arbitrary value for  $m_{tot}$  as one, we can substitute:

$$m_{ini} = [ini] \times m_{TOT} \times \rho \times MW_{ini} = [ini] \times MW_{ini}$$

$$m_{CTA} = \frac{w - ([ini] \times MW_{ini})}{\left( 1 + \frac{DP \times MW_{mon}}{MW_{CTA}} \right)}$$

$$[CTA] = \frac{w - ([ini] \times MW_{ini})}{\left( 1 + \frac{DP \times MW_{mon}}{MW_{CTA}} \right)} \times \frac{1}{MW_{CTA}} = \frac{w - ([ini] \times MW_{ini})}{(DP \times MW_{mon} + MW_{CTA})} \quad (3)$$

The combination of above can be used to conveniently calculate the pair of flow rates required for a given residence time ( $\tau$ ), target DP ( $DP$ ) and the known chemical composition of the two reagent feedstock solutions, described with subscripts A and B. All concentrations are denoted as " $[x]$ " and are used in units of  $mol\ dm^{-3}$ .

$$Q_A = \frac{\frac{V_R}{\tau} \left( \frac{w - ([ini] \times MW_{ini})}{(DP \times MW_{mon} + MW_{CTA})} - [CTA]_B \right)}{[CTA]_A - [CTA]_B} \quad (4)$$

$$Q_B = Q_{TOT} - Q_A \quad (2)$$

These equations were integrated into the MATLAB GUI used to control all the experiments performed using the platform.

It is also important to know the final monomer concentration ( $[M]_f$ ), so that an accurate conversion can be calculated from the NMR spectrum generated. This can be found simply by use of

$$x_A Q_A + x_B Q_B = x_{TOT} Q_{TOT}$$

Where if we consider  $x$  in this case to represent the concentration of monomer, then the total concentration of monomer is given by

$$\frac{x_A Q_A + x_B Q_B}{Q_{TOT}} = x_{TOT} \quad (5)$$

## Conversion methodology

Benchtop  $^1\text{H}$  NMR spectroscopy uses a fixed receiver gain and therefore the integral of signal is directly proportional to the concentration of protons in a given volume. In this case, the same region of flow cell is maintained throughout, meaning volume is constant. This enables the calculation of conversion from a single region, with no requirement for normalisation of signal. A calibration curve was produced to elucidate the relationship between monomer concentration and the integral for the alkenyl protons at 6.6-5.3 ppm. This enables forward prediction of the integral that would be expected for a given target DP at  $t = 0$ , which can be inserted into Equation (6) to yield conversion.

The platform was operated in the same fashion as for the main experiments, with two mixed streams: two "dummy" reactant solutions were formulated without initiator and loaded onto the platform. Using Equations (2) & (4), the appropriate pair of flow rates were calculated for a range of 10 monomer concentrations between  $2.85 \times 10^{-4} \text{ mol dm}^{-3}$  and  $4.2 \times 10^{-4} \text{ mol dm}^{-3}$ . These conditions loaded to the pumps and the system brought to steady state, before 3 NMR spectra were collected and the integral between 5.3 and 6.6 measured (black squares, Figure S4). Prior to the screening experiment, individual  $t_0$  experiments for the four target DPs were performed, and these can be used as a validation for this approach, and indeed they show the predictive power of the calibration curve (blue crossed circles, Figure S4), by each falling on or very near to the line.

**Table S1.** Flow rates to achieve desired monomer concentrations from  $2.85 \times 10^{-4} \text{ mol dm}^{-3}$  to  $4.2 \times 10^{-4} \text{ mol dm}^{-3}$

| Target [M] / mol dm <sup>-3</sup> | Q <sub>A</sub> / ml min <sup>-1</sup> | Q <sub>B</sub> / ml min <sup>-1</sup> |
|-----------------------------------|---------------------------------------|---------------------------------------|
| $2.85 \times 10^4$                | 0.970                                 | 0.030                                 |
| $3 \times 10^4$                   | 0.873                                 | 0.127                                 |
| $3.15 \times 10^4$                | 0.775                                 | 0.225                                 |
| $3.3 \times 10^4$                 | 0.677                                 | 0.323                                 |
| $3.45 \times 10^4$                | 0.580                                 | 0.420                                 |
| $3.6 \times 10^4$                 | 0.482                                 | 0.518                                 |
| $3.75 \times 10^4$                | 0.384                                 | 0.616                                 |
| $3.9 \times 10^4$                 | 0.287                                 | 0.713                                 |
| $4.05 \times 10^4$                | 0.189                                 | 0.811                                 |
| $4.2 \times 10^4$                 | 0.091                                 | 0.909                                 |

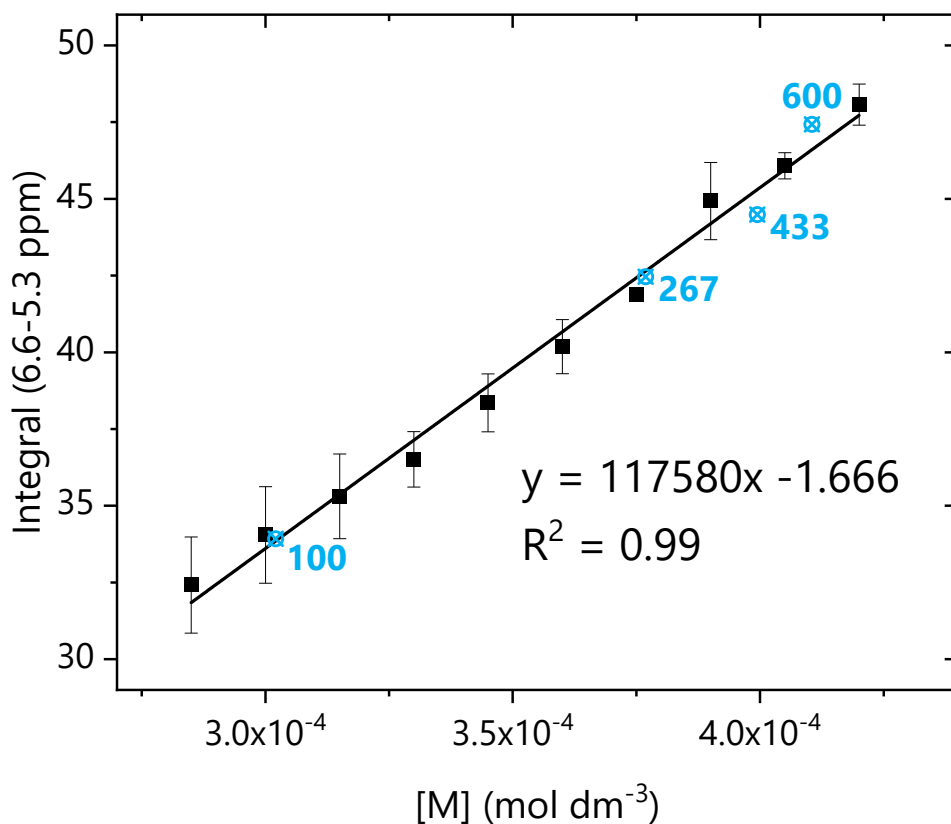


**Figure S4.** Calibration curve relating the alkenyl integral at 6.6-5.3 ppm to the monomer concentration ( $[M]$ ). Each point is the average of three measurements, with error bars indicating the minimum and maximum values obtained for each of the three. The blue crossed circles show the integral value obtained for  $t_0$  samples for each of the four levels of the  $4 \times 4 \times 4$  screen using the reagent solutions prior to the screen. Their proximity to the calibration curve demonstrates the applicability of this approach. Inset: The equation for the calibration curve and  $R^2$  value.

As shown on the graph, the calibration equation is

$$y = 1.18 \times 10^6 \cdot x - 1.666$$

Where  $x$  is given as the concentration of monomer as calculated by Equation (5).

We can then insert this into the conventional conversion equation to calculate the conversion from any given integral,

$$\alpha = 1 - \frac{[M]}{[M]_0} = 1 - \frac{\text{int}_m}{1.18 \times 10^6 \cdot x - 1.666} \quad (6)$$

where  $x$  is the calculated monomer concentration for the reaction mixture assuming no reaction has taken place.

## Materials

2,2-azobis(2-methylpropionitrile) (AIBN, 98 %), dimethylacrylamide (DMAm, 99 %), 1,4-dioxane, diethyl ether (Sigma-Aldrich (UK)); 2,2'-Azobis[2-(2-imidazolin-2-yl)propane]dihydr-ochloride (VA-044, Wako Speciality Chemicals); diacetone acrylamide (DAAm, 99 %, Alfa Aesar); 2-(Butylthiocarbonothioylthio)propanoic acid (TTC-1, ≥95 %, Boron Molecular (Raleigh, USA)), were all used as supplied.

## Methods

### Synthesis of PDMA<sub>x</sub> macro chain transfer agent (macro-CTA)

AIBN (21.6 mg, 0.13 mmol), TTC-1 (0.60 g, 2.51 mmol) and DMAm (24.9 g, 0.251 mol) were dissolved with stirring in 61.6 mL 1,4-dioxane for a 30 % solids (w/w) solution which was sealed and sparged with N<sub>2</sub> for 30 minutes. The solution was heated with stirring to 70 °C for 46 minutes, to target a conversion of 75 %, after which it was cooled to room temperature and then exposed to air to quench further reaction. The resulting polymer was precipitated from solution by dropping into vigorously stirred diethyl ether (1.4 L) and dried under reduced pressure to yield PDMA<sub>75</sub> in run 1 and PDMA<sub>74</sub> in run 2, as determined by <sup>1</sup>H NMR, assuming all conversion of monomer yielded polymer.

### Automated RAFT polymerisation

VA-044, PDMA<sub>x</sub> macro-CTA (macro-chain transfer agent) and DAAm were loaded into two reservoir solutions in ratios to approximately target degrees of polymerisation (DP) of 80 and 2500 respectively and dissolved in pH 2.5 water at 7.5 % solids (w/w). E.g. **Reservoir 1** (Target DP = 80) : VA-044 (20.7 mg, 0.06 mmol), PDMA<sub>75</sub> macro-CTA (2.31 g, 0.30 mmol) and DAAm (4.06 g, 24.0 mmol) in 79 mL pH 2.5 water; **Reservoir 2** (Target DP = 2495): VA-044 (46.7 mg, 0.14 mmol), PDMA<sub>75</sub> macro-CTA (0.261 g, 0.30 mmol) and DAAm (14.30 g, 84.5 mmol) in 180 mL pH 2.5 water. For each experiment approximately 10.5 mL in total was used (2 mL initial purge, 7 mL for steady state, 1.5 mL for analysis), with the appropriate flow rates from each reservoir calculated to target a particular DP.

### Detailed experimental protocol for optimisation experiments

VA-044, PDMA<sub>x</sub> macro-CTA and DAAm were loaded into two reservoir solutions in ratios to approximately target degrees of polymerisation of 80 and 2500 respectively and dissolved in pH 2.5 water. Each delivery pump is then primed with the material. The chemical information for the formulation used was loaded to the GUI, in order that the appropriate flow rates for a target DP can be calculated, as well as the total monomer concentration, that conversion can be calculated from the calibration curve. The limits (min/max/step size) of the experiment in terms of input variables were then provided the platform and the experiment started.

For each experiment iteration within an automated experiment, the experimental protocol is as follows: for the given conditions (by full factorial sampling, initial Latin Hypercube sampling or algorithmic selection), the reactor is brought to the correct temperature, and the appropriate flow rates calculated as per Equations (2) & (4). After reaching the selected temperature, the reaction mixtures were pumped at the same ratio to that calculated for the experiment but scaled to a total flow rate of 1 ml min<sup>-1</sup>, for an initialisation period of two minutes. This facilitated the equilibration of the output of the mixer (i.e. at the appropriate

ratio for the given experiment) and aided the clearing out of the reactor after the previous experiment. Following this, the flow rates were then reduced to the appropriate flow rates for the required residence time. These conditions were maintained for 3.5 times the residence time and then the analytical element of the experiment performed.

First, the GPC analysis would be started, with the triggering of the sample loop. The GPC analysis used three injections and upon the third injection, the flow was altered (again maintaining the flow ratio for the experiment) to  $0.1 \text{ ml min}^{-1}$ . The NMR and DLS analyses loops were then started. For the NMR, the spectrometer would first perform a "shim on sample" and then the NMR experiment proper – using the presaturation routine described above. For the DLS, the appropriate sample loop (SL2) was switched to direct the flow through the DLS flow cell and then the DLS dilution pump turned on at  $5 \text{ ml min}^{-1}$  for 30 seconds. The flow was then redirected, and the dilution pump switched off. The analysis was performed as described above, and upon the completion of all three analyses, the next iteration of the loop was triggered, again by selecting the experimental conditions and setting the reactor temperature.

The maximum number of iterations was set at 15 for each algorithmically driven element, with each experiment using the same initial 15 LHS starting experiments, making each "optimisation" 30 experiments in total. The data was passed to the algorithms as input / output pairs of conditions selected / results obtained, with particle size converted to a size objective via a loss function to target a particle size of 80 nm:

$$\text{Size Objective} = \left( \frac{\text{Size} - \text{Target Size}}{\text{Target Size}} \right)^2$$

**Equation S1.** Loss function used for size targeting as part of the optimisation campaigns

For TSEMO this was performed in MATLAB, and the objectives were passed as the natural logarithm of the values, as advised in the original use case. For RBFNN/RVEA and EA-MOPSO, input/output pairs and new inputs were passed via .txt files uploaded to a shared cloud-based directory.

### Algorithmic application

TSEMO is a well-established algorithm and was used in MATLAB, as available here, <https://github.com/Eric-Bradford/TS-EMO><sup>2,3</sup>

The RBFNN/RVEA was applied based upon code modified from PlatEMO,<sup>4</sup> in ask-tell mode.

EA-MOPSO was applied as described in previous work,<sup>5</sup> in ask-tell mode.

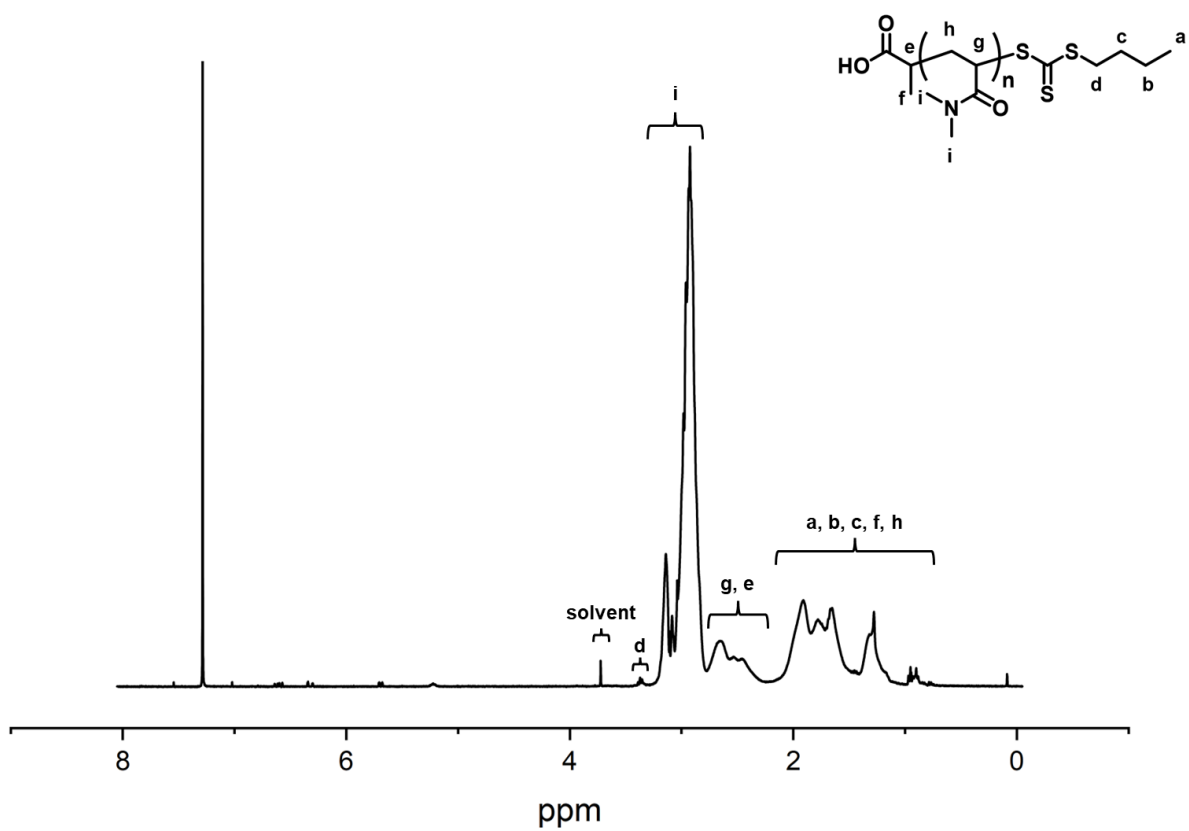


**Figure S5.** Assigned  $^1\text{H}$  NMR spectrum for the PDMAm<sub>75</sub> macro-CTA used in this work

## Automated experiment results

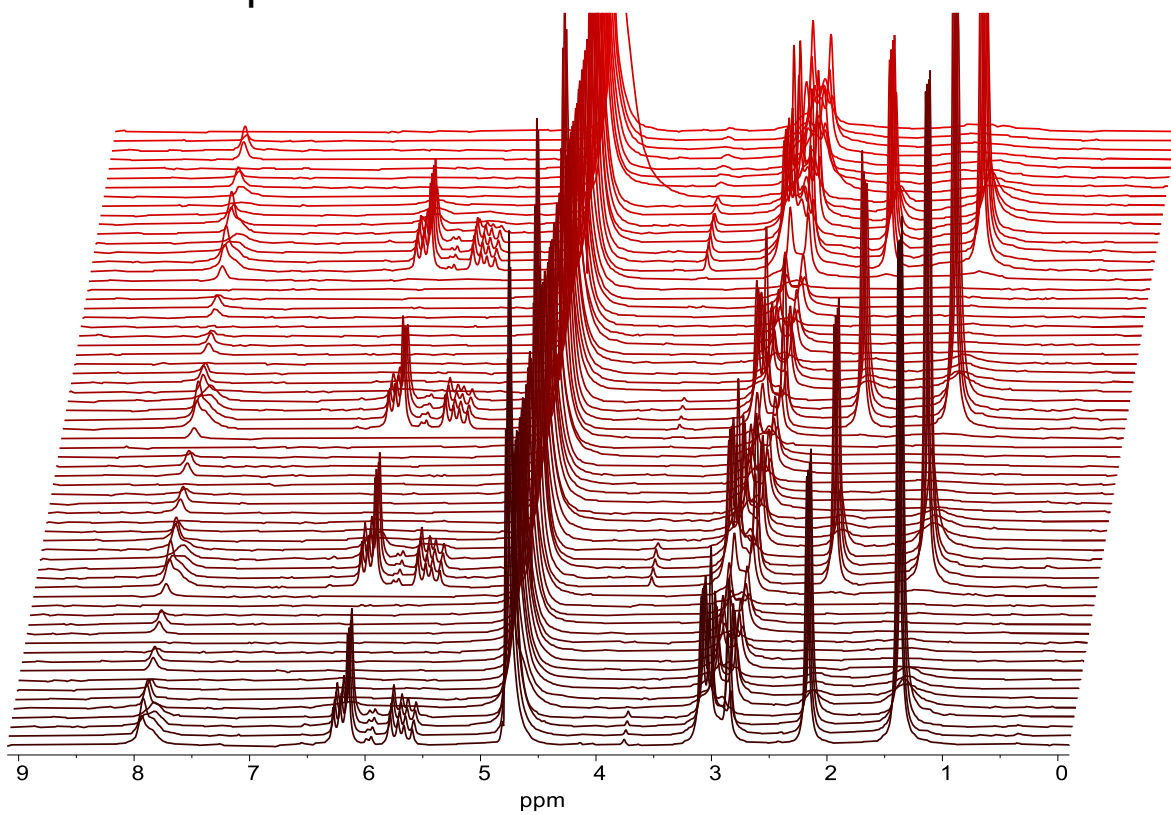


**Figure S6.** <sup>1</sup>H NMR spectra for the 4 x 4 x 4 screen for the RAFT dispersion polymerisation of DAAm in pH 2.5 water, using PDMA<sub>74</sub> as the macro-chain transfer agent and VA-044 as the initiator.

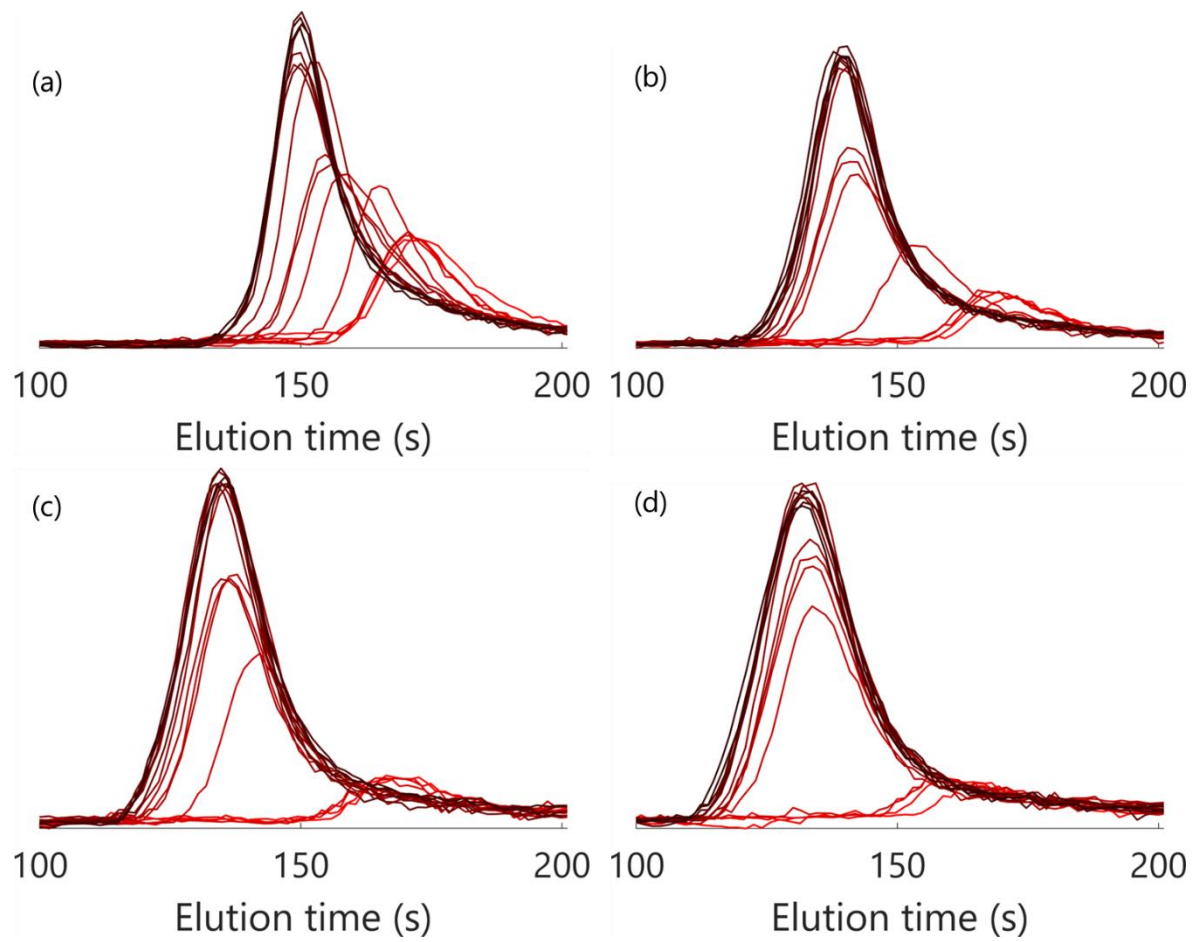


**Figure S7.** Raw chromatograms from GPC in the  $4 \times 4 \times 4$  screen for the four levels of  $[M]:[CTA]$ : (a) 100, (b) 267, (c) 433 and (d) 600 for the RAFT dispersion polymerisation of DAAm in pH 2.5 water, using PDMA<sub>74</sub> as the macro-chain transfer agent and VA-044 as the initiator.

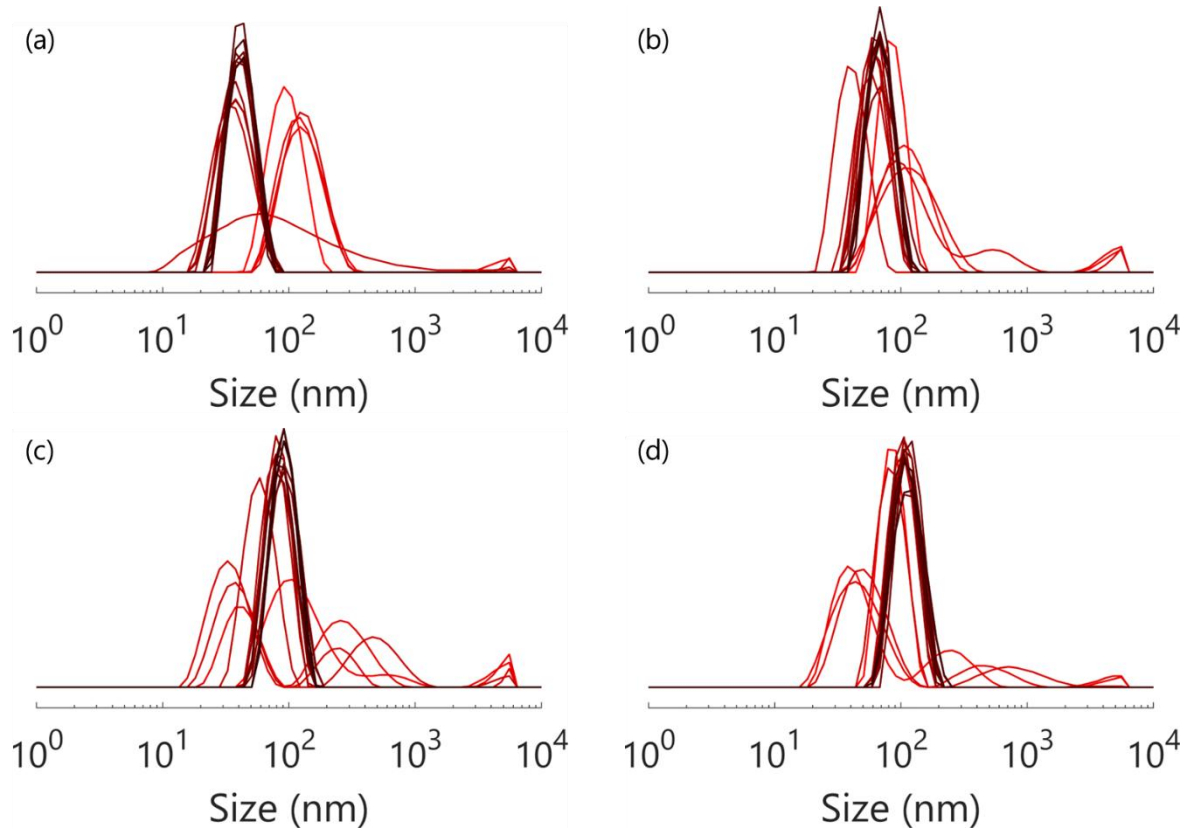


**Figure S8.** Intensity particle size distributions from DLS in the  $4 \times 4 \times 4$  screen for the four levels of  $[M]:[CTA]$ : (a) 100, (b) 267, (c) 433 and (d) 600 for the RAFT dispersion polymerisation of DAAm in pH 2.5 water, using PDMA<sub>74</sub> as the macro-chain transfer agent and VA-044 as the initiator.

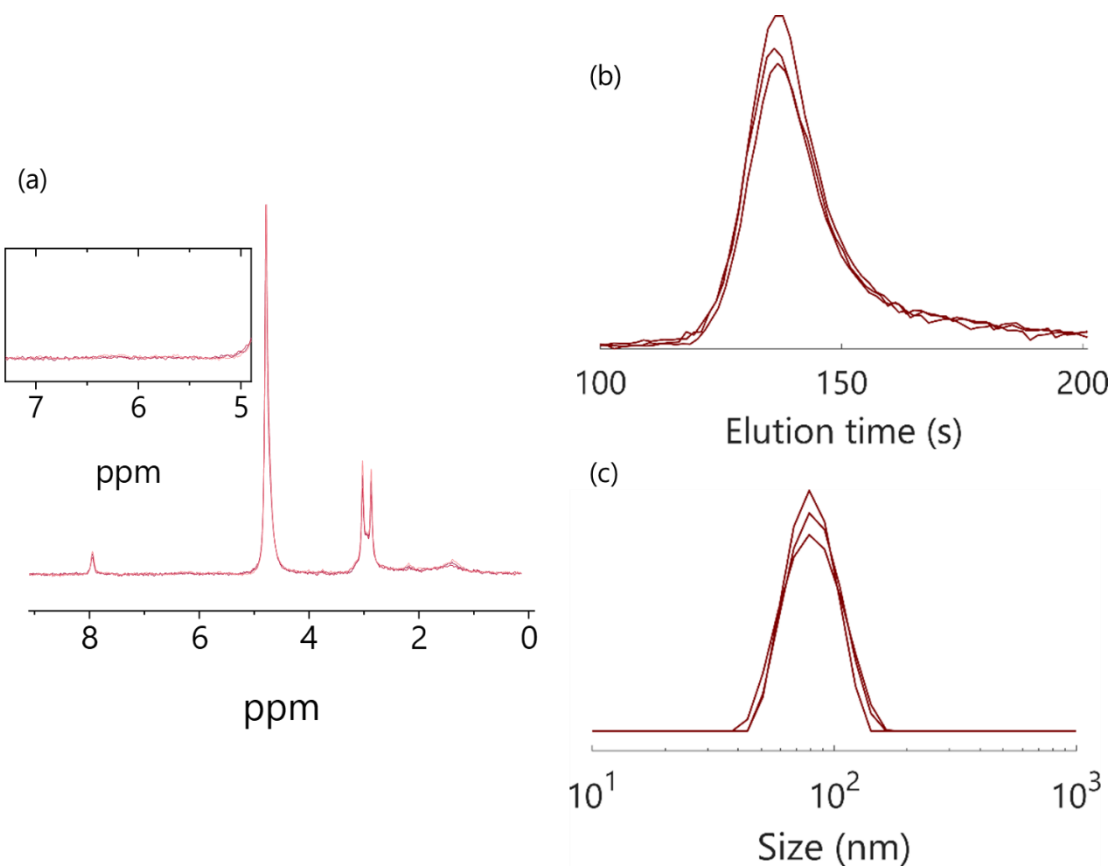


**Figure S9.** (a) <sup>1</sup>H NMR spectra, (b) Raw GPC chromatograms and (c) DLS intensity particle size distributions for the three repeats at the centre point (17.5 mins, 74 °C, [M]:[CTA] = 350) of the 4 x 4 x 4 full factorial screen for the RAFT dispersion polymerisation of DAAM in pH 2.5 water, using PDMA<sub>74</sub> as the macro-chain transfer agent and VA-044 as the initiator

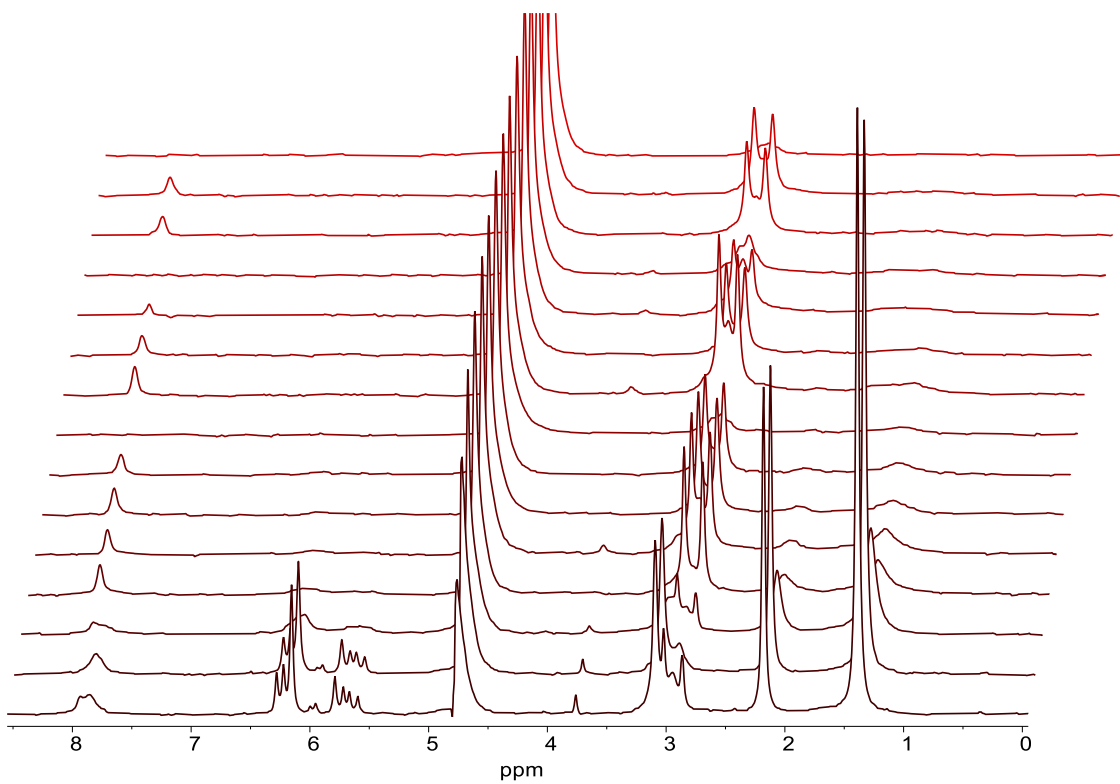


**Figure S10.** NMR spectra for the 15 experiments selected using Latin Hypercube sampling, for the RAFT dispersion polymerisation of DAAm in pH 2.5 water, using PDMA<sub>74</sub> as the macro-chain transfer agent and VA-044 as the initiator.

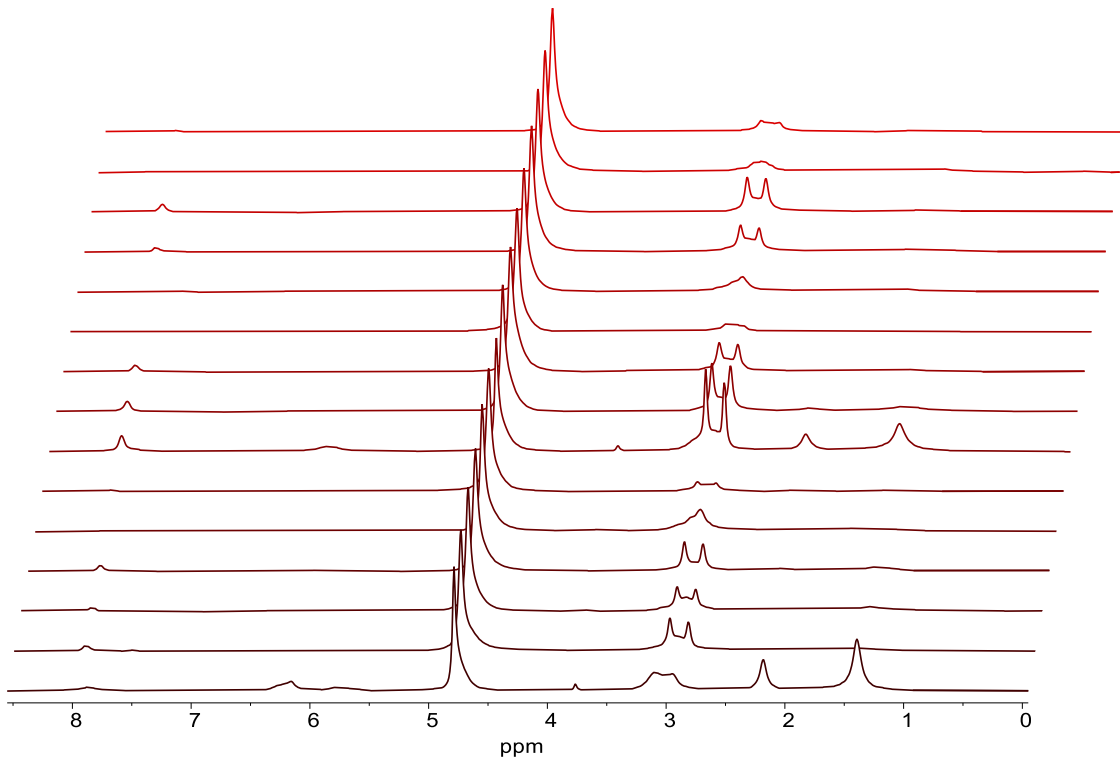


**Figure S11.** NMR spectra for the 15 experiments selected using the TSEMO algorithm, for the RAFT dispersion polymerisation of DAAm in pH 2.5 water, using PDMA<sub>74</sub> as the macro-chain transfer agent and VA-044 as the initiator.

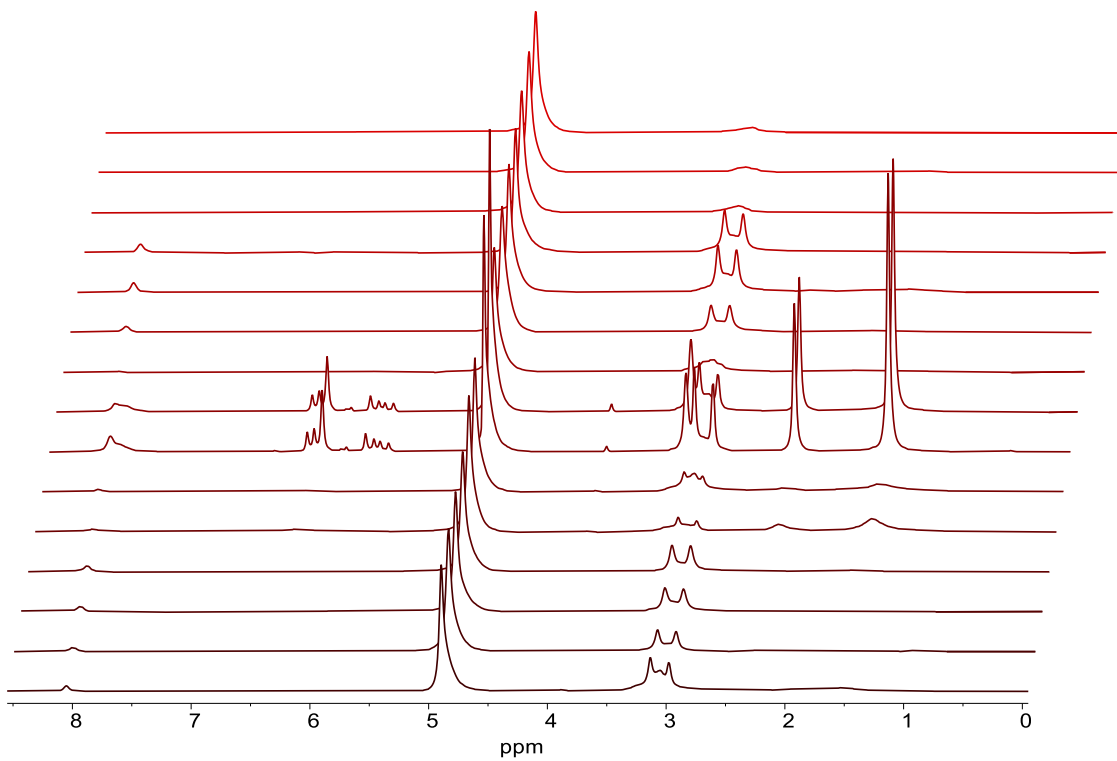


**Figure S12.** NMR spectra for the 15 experiments selected using the RBFNN/RVEA algorithm, for the RAFT dispersion polymerisation of DAAm in pH 2.5 water, using PDMA<sub>74</sub> as the macro-chain transfer agent and VA-044 as the initiator.

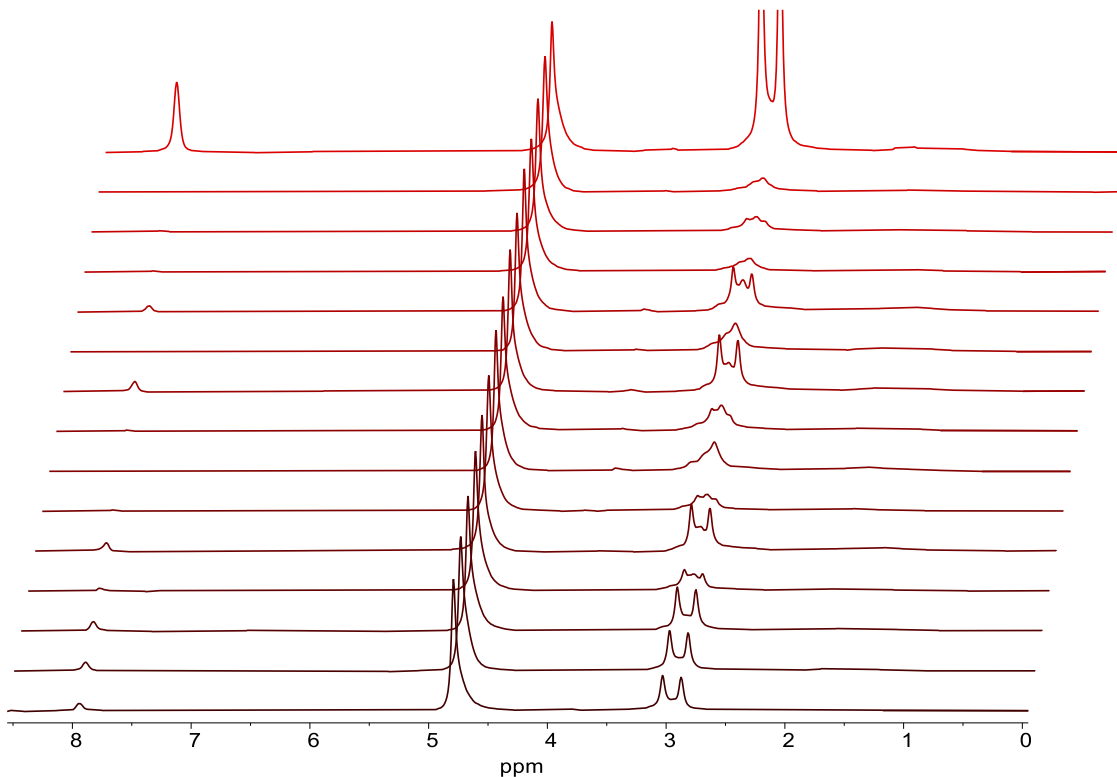


**Figure S13.** NMR spectra for the 15 experiments selected using the MOPSO algorithm, for the RAFT dispersion polymerisation of DAAm in pH 2.5 water, using PDMA<sub>74</sub> as the macro-chain transfer agent and VA-044 as the initiator.

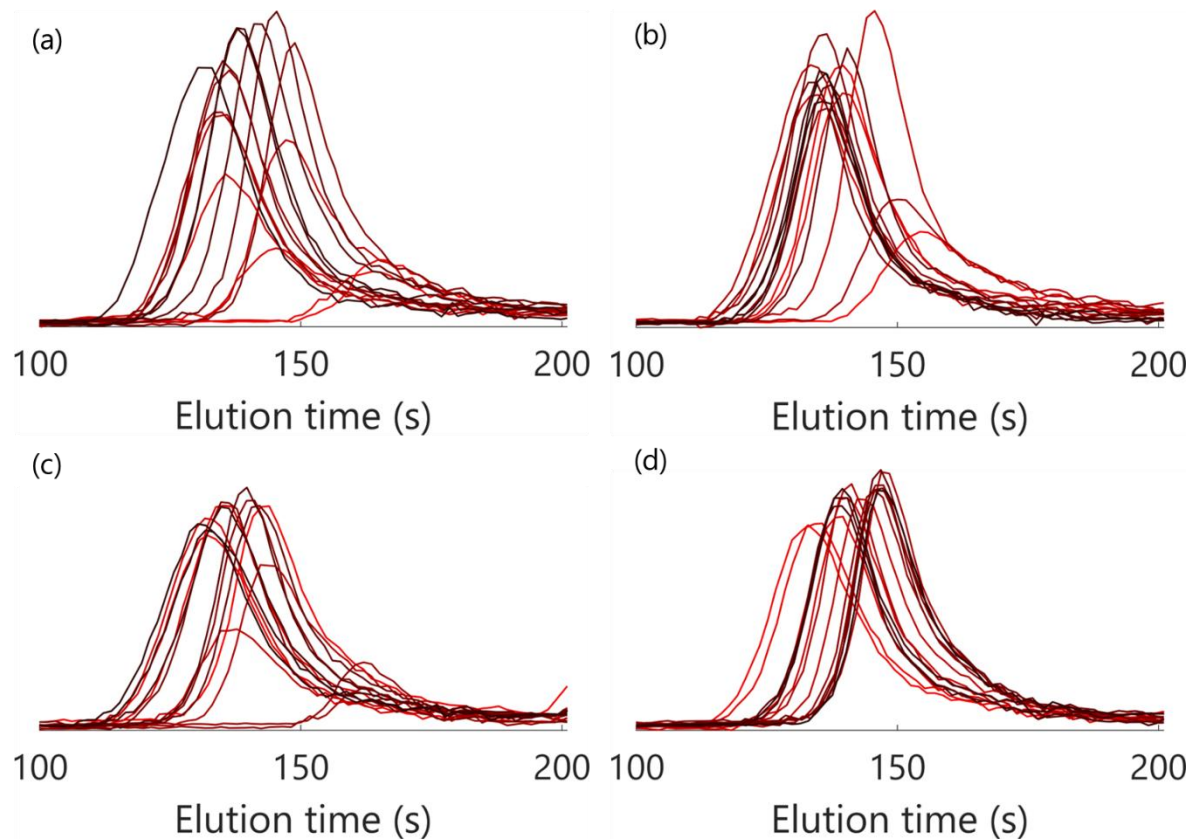


**Figure S14.** GPC chromatograms for (a) the 15 experiments selected using Latin Hypercube sampling, (b) the 15 experiments selected using the TSEMO algorithm, (c) the 15 experiments selected using the RBFNN/RVEA algorithm, and (d) the 15 experiments selected using the MOPSO algorithm; for the RAFT dispersion polymerisation of DAAm in pH 2.5 water, using PDMA<sub>74</sub> as the macro-chain transfer agent and VA-044 as the initiator.

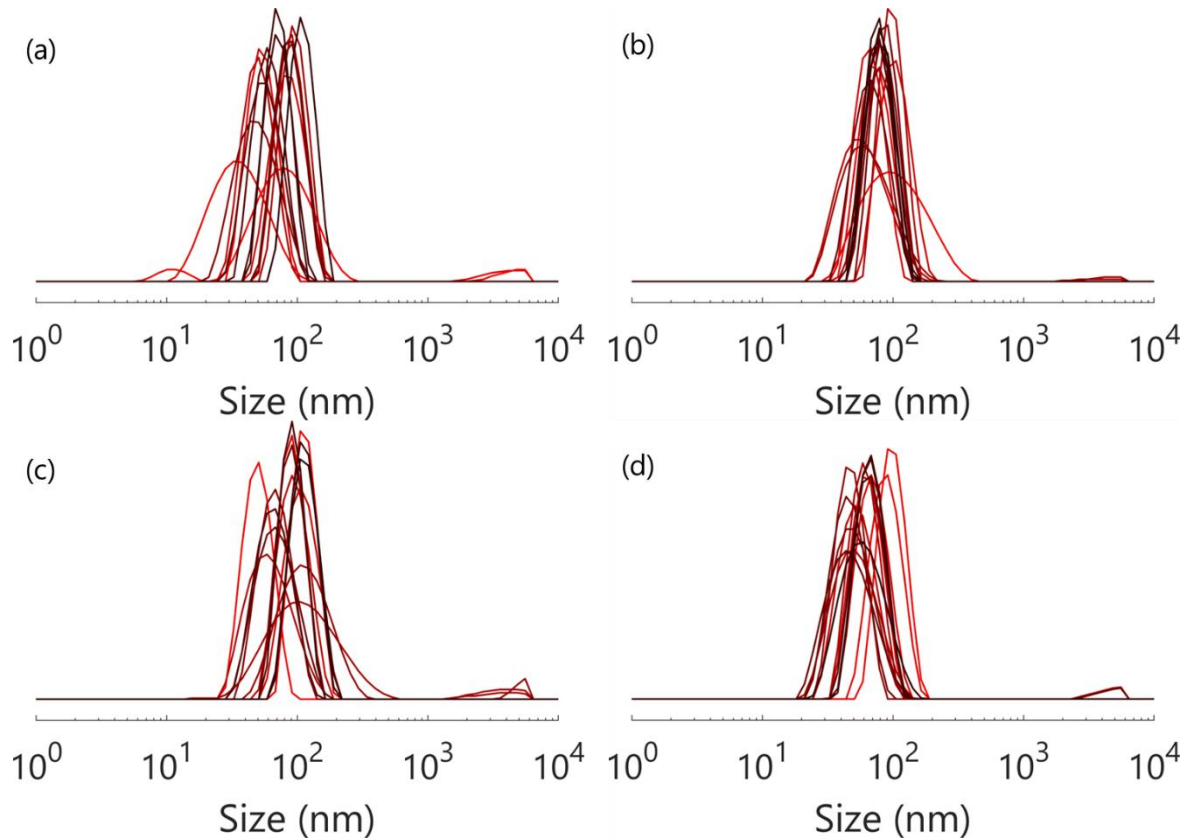


**Figure S15.** Intensity particle size distributions for (a) the 15 experiments selected using Latin Hypercube sampling, (b) the 15 experiments selected using the TSEMO algorithm, (c) the 15 experiments selected using the RBFNN/RVEA algorithm, and (d) the 15 experiments selected using the MOPSO algorithm; for the RAFT dispersion polymerisation of DAAm in pH 2.5 water, using PDMA<sub>74</sub> as the macro-chain transfer agent and VA-044 as the initiator.

**Table S2.** Each of the experiments conducted as part of the high throughput screen (4x4x4 – three **centre-point datapoints shown in bold iterations 17,34,51**), the Latin hypercube sampling (LHS) and the three optimisation campaigns (TSEMO, RVEA, MOPSO)

| Exp   | Iteration | RT     | T    | [M]:[CTA] | Conversion | Dispersity | M <sub>n</sub> | (g mol <sup>-1</sup> ) | M <sub>p</sub> | (g mol <sup>-1</sup> ) | Particle size | PDI |
|-------|-----------|--------|------|-----------|------------|------------|----------------|------------------------|----------------|------------------------|---------------|-----|
|       |           | (mins) | (°C) |           | (%)        |            | (nm)           |                        |                |                        |               |     |
| 4x4x4 | 1         | 6      | 68   | 433       | 1.99       | 1.43       | 6279           | 8497                   | 114.3          | 0.47                   |               |     |
| 4x4x4 | 2         | 14     | 68   | 433       | 3.11       | 1.94       | 6804           | 11484                  | 80.0           | 0.75                   |               |     |
| 4x4x4 | 3         | 22     | 68   | 433       | 0.38       | 1.53       | 7329           | 13459                  | 52.7           | 0.29                   |               |     |
| 4x4x4 | 4         | 30     | 68   | 433       | 8.28       | 2.47       | 7200           | 11513                  | 53.0           | 0.64                   |               |     |
| 4x4x4 | 5         | 6      | 72   | 433       | 74.95      | 1.83       | 61275          | 113784                 | 56.7           | 0.06                   |               |     |
| 4x4x4 | 6         | 14     | 72   | 433       | 92.84      | 1.87       | 108879         | 185965                 | 76.8           | 0.01                   |               |     |
| 4x4x4 | 7         | 22     | 72   | 433       | 90.78      | 1.81       | 109873         | 177078                 | 80.5           | 0.01                   |               |     |
| 4x4x4 | 8         | 30     | 72   | 433       | 93.16      | 1.88       | 116666         | 206145                 | 83.1           | 0.00                   |               |     |
| 4x4x4 | 9         | 6      | 76   | 433       | 99.06      | 1.81       | 142176         | 219062                 | 80.4           | 0.04                   |               |     |
| 4x4x4 | 10        | 14     | 76   | 433       | 99.91      | 1.95       | 145827         | 236508                 | 89.2           | 0.04                   |               |     |
| 4x4x4 | 11        | 22     | 76   | 433       | 99.56      | 2.00       | 135494         | 227031                 | 92.3           | 0.02                   |               |     |
| 4x4x4 | 12        | 30     | 76   | 433       | 96.11      | 1.83       | 153265         | 231361                 | 90.7           | 0.02                   |               |     |
| 4x4x4 | 13        | 6      | 80   | 433       | 98.46      | 1.85       | 148100         | 232987                 | 82.6           | 0.04                   |               |     |
| 4x4x4 | 14        | 14     | 80   | 433       | 99.73      | 2.02       | 164719         | 262680                 | 89.6           | 0.03                   |               |     |
| 4x4x4 | 15        | 22     | 80   | 433       | 95.31      | 2.05       | 141227         | 220779                 | 90.9           | 0.04                   |               |     |
| 4x4x4 | 16        | 30     | 80   | 433       | 96.38      | 2.14       | 149743         | 254185                 | 91.3           | 0.01                   |               |     |
| 4x4x4 | 18        | 6      | 68   | 267       | 3.44       | 1.81       | 6138           | 7914                   | 82.3           | 0.02                   |               |     |
| 4x4x4 | 19        | 14     | 68   | 267       | 4.62       | 1.30       | 7004           | 10919                  | 108.3          | 0.30                   |               |     |
| 4x4x4 | 20        | 22     | 68   | 267       | 8.30       | 1.34       | 6706           | 10428                  | 114.2          | 0.35                   |               |     |
| 4x4x4 | 21        | 30     | 68   | 267       | 0.80       | 1.31       | 6938           | 11103                  | 112.4          | 0.53                   |               |     |
| 4x4x4 | 22        | 6      | 72   | 267       | 47.80      | 1.55       | 18239          | 30422                  | 39.0           | 0.08                   |               |     |
| 4x4x4 | 23        | 14     | 72   | 267       | 79.04      | 1.82       | 50773          | 96553                  | 56.2           | 0.04                   |               |     |
| 4x4x4 | 24        | 22     | 72   | 267       | 89.51      | 1.73       | 59843          | 104041                 | 58.1           | 0.05                   |               |     |

|       |    |    |    |     |       |      |        |        |       |      |
|-------|----|----|----|-----|-------|------|--------|--------|-------|------|
| 4x4x4 | 25 | 30 | 72 | 267 | 92.10 | 1.75 | 64032  | 110079 | 60.0  | 0.05 |
| 4x4x4 | 26 | 6  | 76 | 267 | 98.74 | 1.55 | 86594  | 124116 | 62.3  | 0.01 |
| 4x4x4 | 27 | 14 | 76 | 267 | 99.99 | 1.63 | 86621  | 142833 | 66.3  | 0.07 |
| 4x4x4 | 28 | 22 | 76 | 267 | 98.90 | 1.65 | 91597  | 145715 | 68.1  | 0.00 |
| 4x4x4 | 29 | 30 | 76 | 267 | 97.70 | 1.60 | 96880  | 145487 | 68.6  | 0.01 |
| 4x4x4 | 30 | 6  | 80 | 267 | 99.99 | 1.52 | 92746  | 129777 | 64.9  | 0.04 |
| 4x4x4 | 31 | 14 | 80 | 267 | 99.26 | 1.63 | 100815 | 159315 | 66.6  | 0.02 |
| 4x4x4 | 32 | 22 | 80 | 267 | 99.99 | 1.62 | 91897  | 134200 | 68.1  | 0.02 |
| 4x4x4 | 33 | 30 | 80 | 267 | 95.17 | 1.63 | 96501  | 142911 | 67.8  | 0.03 |
| 4x4x4 | 35 | 6  | 68 | 600 | 8.08  | 2.33 | 7404   | 12060  | 84.0  | 0.01 |
| 4x4x4 | 36 | 14 | 68 | 600 | 14.26 | 2.36 | 8431   | 18955  | 53.2  | 0.36 |
| 4x4x4 | 37 | 22 | 68 | 600 | 13.84 | 1.82 | 8085   | 21271  | 53.8  | 0.36 |
| 4x4x4 | 38 | 30 | 68 | 600 | 16.33 | 2.61 | 8163   | 23826  | 57.4  | 0.34 |
| 4x4x4 | 39 | 6  | 72 | 600 | 86.70 | 1.98 | 130691 | 227329 | 81.2  | 0.04 |
| 4x4x4 | 40 | 14 | 72 | 600 | 92.88 | 2.20 | 151668 | 304847 | 99.7  | 0.02 |
| 4x4x4 | 41 | 22 | 72 | 600 | 93.09 | 2.21 | 161848 | 268579 | 105.4 | 0.08 |
| 4x4x4 | 42 | 30 | 72 | 600 | 95.00 | 2.23 | 170844 | 320845 | 108.2 | 0.00 |
| 4x4x4 | 43 | 6  | 76 | 600 | 96.34 | 2.07 | 185180 | 304593 | 101.1 | 0.02 |
| 4x4x4 | 44 | 14 | 76 | 600 | 99.99 | 2.22 | 186258 | 373441 | 110.1 | 0.04 |
| 4x4x4 | 45 | 22 | 76 | 600 | 97.00 | 2.17 | 189299 | 373651 | 109.6 | 0.04 |
| 4x4x4 | 46 | 30 | 76 | 600 | 97.39 | 2.09 | 194311 | 347496 | 116.3 | 0.00 |
| 4x4x4 | 47 | 6  | 80 | 600 | 99.74 | 2.15 | 180530 | 320901 | 103.2 | 0.03 |
| 4x4x4 | 48 | 14 | 80 | 600 | 98.57 | 2.19 | 180881 | 380693 | 106.0 | 0.04 |
| 4x4x4 | 49 | 22 | 80 | 600 | 95.19 | 2.20 | 182126 | 351544 | 109.3 | 0.03 |
| 4x4x4 | 50 | 30 | 80 | 600 | 97.28 | 2.25 | 176241 | 320775 | 111.8 | 0.05 |
| 4x4x4 | 52 | 6  | 68 | 100 | 2.49  | 1.18 | 6211   | 8435   | 89.1  | 0.08 |
| 4x4x4 | 53 | 14 | 68 | 100 | 2.34  | 1.17 | 6788   | 9118   | 122.1 | 0.25 |
| 4x4x4 | 54 | 22 | 68 | 100 | 6.29  | 1.19 | 6986   | 8777   | 112.4 | 0.17 |
| 4x4x4 | 55 | 30 | 68 | 100 | 5.71  | 1.19 | 7216   | 9591   | 123.4 | 0.34 |
| 4x4x4 | 56 | 6  | 72 | 100 | 21.11 | 1.15 | 10586  | 13795  | 52.8  | 0.46 |

|              |           |           |           |            |              |             |               |               |             |             |
|--------------|-----------|-----------|-----------|------------|--------------|-------------|---------------|---------------|-------------|-------------|
| 4x4x4        | 57        | 14        | 72        | 100        | 63.72        | 1.34        | 14122         | 22586         | 34.4        | 0.15        |
| 4x4x4        | 58        | 22        | 72        | 100        | 68.01        | 1.38        | 16753         | 27476         | 36.0        | 0.09        |
| 4x4x4        | 59        | 30        | 72        | 100        | 69.37        | 1.42        | 16816         | 28567         | 36.3        | 0.09        |
| 4x4x4        | 60        | 6         | 76        | 100        | 94.21        | 1.28        | 25783         | 34269         | 35.7        | 0.07        |
| 4x4x4        | 61        | 14        | 76        | 100        | 99.99        | 1.38        | 30297         | 45417         | 39.4        | 0.06        |
| 4x4x4        | 62        | 22        | 76        | 100        | 96.43        | 1.37        | 31003         | 47959         | 40.6        | 0.04        |
| 4x4x4        | 63        | 30        | 76        | 100        | 96.07        | 1.37        | 30759         | 46333         | 40.8        | 0.05        |
| 4x4x4        | 64        | 6         | 80        | 100        | 99.99        | 1.29        | 34979         | 47435         | 38.7        | 0.06        |
| 4x4x4        | 65        | 14        | 80        | 100        | 99.99        | 1.28        | 33124         | 45404         | 41.1        | 0.02        |
| 4x4x4        | 66        | 22        | 80        | 100        | 97.84        | 1.31        | 33815         | 43611         | 41.2        | 0.02        |
| 4x4x4        | 67        | 30        | 80        | 100        | 96.04        | 1.30        | 33061         | 44654         | 41.4        | 0.06        |
| <b>4x4x4</b> | <b>17</b> | <b>18</b> | <b>74</b> | <b>350</b> | <b>98.55</b> | <b>1.73</b> | <b>116848</b> | <b>191458</b> | <b>78.0</b> | <b>0.06</b> |
| <b>4x4x4</b> | <b>34</b> | <b>18</b> | <b>74</b> | <b>350</b> | <b>97.80</b> | <b>1.74</b> | <b>122028</b> | <b>194594</b> | <b>78.5</b> | <b>0.00</b> |
| <b>4x4x4</b> | <b>51</b> | <b>18</b> | <b>74</b> | <b>350</b> | <b>94.83</b> | <b>1.79</b> | <b>108392</b> | <b>177987</b> | <b>79.8</b> | <b>0.04</b> |
| LHS          | 1         | 21        | 69        | 258        | 8.92         | 1.28        | 8378          | 12546         | 67.9        | 0.30        |
| LHS          | 2         | 28        | 69        | 358        | 11.90        | 1.62        | 7957          | 16422         | 34.5        | 0.26        |
| LHS          | 3         | 22        | 70        | 443        | 52.00        | 2.51        | 23768         | 76525         | 51.9        | 0.04        |
| LHS          | 4         | 16        | 71        | 570        | 80.41        | 2.16        | 106428        | 228369        | 82.1        | 0.05        |
| LHS          | 5         | 18        | 72        | 169        | 86.42        | 1.72        | 30231         | 59601         | 48.6        | 0.04        |
| LHS          | 6         | 8         | 73        | 516        | 94.30        | 1.94        | 154767        | 243785        | 86.4        | 0.02        |
| LHS          | 7         | 15        | 73        | 495        | 92.90        | 2.13        | 137601        | 240381        | 93.4        | 0.01        |
| LHS          | 8         | 28        | 74        | 392        | 99.99        | 1.88        | 134445        | 224357        | 85.7        | 0.07        |
| LHS          | 9         | 11        | 75        | 115        | 99.79        | 1.44        | 33075         | 48515         | 46.5        | 0.13        |
| LHS          | 10        | 10        | 75        | 405        | 99.99        | 1.81        | 136801        | 221406        | 84.5        | 0.02        |
| LHS          | 11        | 20        | 77        | 142        | 99.99        | 1.40        | 49755         | 67620         | 53.3        | 0.07        |
| LHS          | 12        | 25        | 77        | 206        | 99.99        | 1.50        | 71369         | 109696        | 58.1        | 0.05        |
| LHS          | 13        | 13        | 78        | 292        | 97.53        | 1.63        | 102730        | 161273        | 70.0        | 0.02        |
| LHS          | 14        | 7         | 79        | 301        | 98.89        | 1.61        | 106536        | 160282        | 69.6        | 0.01        |
| LHS          | 15        | 27        | 80        | 562        | 95.25        | 2.11        | 200567        | 386715        | 106.6       | 0.01        |
| TSEMO        | 1         | 27        | 70        | 275        | 52.34        | 1.66        | 14706         | 28554         | 90.5        | 0.19        |

|       |    |    |    |     |       |      |        |        |       |      |
|-------|----|----|----|-----|-------|------|--------|--------|-------|------|
| TSEMO | 2  | 14 | 74 | 370 | 97.71 | 1.68 | 86250  | 138703 | 70.9  | 0.03 |
| TSEMO | 3  | 22 | 73 | 253 | 95.22 | 1.61 | 82413  | 132890 | 63.9  | 0.05 |
| TSEMO | 4  | 21 | 73 | 539 | 97.35 | 2.05 | 174329 | 292408 | 98.5  | 0.05 |
| TSEMO | 5  | 28 | 78 | 135 | 99.86 | 1.33 | 50577  | 69075  | 55.6  | 0.15 |
| TSEMO | 6  | 23 | 79 | 482 | 98.42 | 2.18 | 165424 | 276985 | 96.4  | 0.03 |
| TSEMO | 7  | 11 | 71 | 221 | 65.27 | 1.84 | 18872  | 41087  | 59.0  | 0.18 |
| TSEMO | 8  | 15 | 73 | 336 | 92.04 | 1.74 | 115330 | 184752 | 75.4  | 0.09 |
| TSEMO | 9  | 18 | 78 | 357 | 99.99 | 1.70 | 146338 | 196692 | 81.5  | 0.04 |
| TSEMO | 10 | 25 | 78 | 375 | 93.24 | 1.73 | 192450 | 293838 | 85.3  | 0.04 |
| TSEMO | 11 | 30 | 79 | 201 | 97.78 | 1.38 | 89741  | 119204 | 64.7  | 0.07 |
| TSEMO | 12 | 20 | 75 | 302 | 99.19 | 1.52 | 132615 | 191775 | 74.4  | 0.02 |
| TSEMO | 13 | 9  | 78 | 333 | 99.53 | 1.66 | 144279 | 225239 | 77.5  | 0.04 |
| TSEMO | 14 | 27 | 75 | 296 | 99.18 | 1.59 | 145216 | 203884 | 76.2  | 0.02 |
| TSEMO | 15 | 23 | 78 | 327 | 98.27 | 1.58 | 153084 | 205093 | 78.9  | 0.01 |
| RVEA  | 1  | 20 | 76 | 150 | 97.08 | 1.62 | 50028  | 80783  | 48.5  | 0.04 |
| RVEA  | 2  | 20 | 76 | 572 | 96.84 | 2.05 | 189633 | 344792 | 111.0 | 0.00 |
| RVEA  | 3  | 6  | 80 | 449 | 98.12 | 2.13 | 140443 | 247615 | 88.8  | 0.02 |
| RVEA  | 4  | 7  | 79 | 598 | 98.94 | 2.08 | 186961 | 363153 | 103.2 | 0.06 |
| RVEA  | 5  | 30 | 71 | 573 | 75.23 | 2.58 | 67793  | 169071 | 89.1  | 0.09 |
| RVEA  | 6  | 24 | 73 | 173 | 89.90 | 1.70 | 38768  | 84304  | 61.7  | 0.22 |
| RVEA  | 7  | 7  | 68 | 368 | 6.67  | 1.32 | 10915  | 16327  | 100.1 | 0.28 |
| RVEA  | 8  | 20 | 69 | 234 | 11.27 | 1.22 | 12723  | 15925  | 112.2 | 0.31 |
| RVEA  | 9  | 27 | 76 | 232 | 95.98 | 1.63 | 86593  | 133055 | 64.9  | 0.07 |
| RVEA  | 10 | 18 | 78 | 418 | 99.99 | 1.89 | 151052 | 265560 | 87.7  | 0.04 |
| RVEA  | 11 | 15 | 75 | 208 | 97.97 | 1.60 | 67989  | 119892 | 65.5  | 0.13 |
| RVEA  | 12 | 16 | 76 | 225 | 99.99 | 1.63 | 79266  | 135157 | 62.8  | 0.08 |
| RVEA  | 13 | 30 | 80 | 408 | 93.83 | 2.18 | 144055 | 245049 | 89.8  | 0.00 |
| RVEA  | 14 | 28 | 79 | 548 | 94.31 | 2.27 | 166513 | 397245 | 108.6 | 0.05 |
| RVEA  | 15 | 30 | 80 | 544 | 93.74 | 2.20 | 186005 | 350318 | 110.5 | 0.02 |
| MOPSO | 1  | 7  | 76 | 498 | 99.41 | 2.09 | 170528 | 298254 | 96.5  | 0.00 |

|       |    |    |    |     |       |      |        |        |      |      |
|-------|----|----|----|-----|-------|------|--------|--------|------|------|
| MOPSO | 2  | 11 | 75 | 399 | 99.13 | 1.98 | 140023 | 235133 | 85.7 | 0.04 |
| MOPSO | 3  | 7  | 75 | 293 | 99.84 | 1.63 | 98097  | 154764 | 67.0 | 0.05 |
| MOPSO | 4  | 22 | 77 | 205 | 99.53 | 1.56 | 73467  | 117474 | 61.6 | 0.04 |
| MOPSO | 5  | 18 | 76 | 145 | 98.41 | 1.54 | 52358  | 94494  | 50.3 | 0.10 |
| MOPSO | 6  | 24 | 79 | 199 | 99.99 | 1.51 | 74937  | 115056 | 58.8 | 0.03 |
| MOPSO | 7  | 30 | 80 | 100 | 99.99 | 1.38 | 37505  | 61012  | 50.5 | 0.21 |
| MOPSO | 8  | 24 | 77 | 119 | 99.99 | 1.42 | 44832  | 68642  | 45.8 | 0.03 |
| MOPSO | 9  | 17 | 77 | 117 | 99.00 | 1.43 | 40854  | 63460  | 45.9 | 0.11 |
| MOPSO | 10 | 27 | 78 | 107 | 99.83 | 1.37 | 41119  | 59464  | 43.5 | 0.07 |
| MOPSO | 11 | 19 | 78 | 100 | 99.99 | 1.35 | 39074  | 60660  | 46.1 | 0.20 |
| MOPSO | 12 | 28 | 79 | 243 | 99.99 | 1.61 | 100857 | 140384 | 64.8 | 0.04 |
| MOPSO | 13 | 25 | 76 | 225 | 97.58 | 1.59 | 83960  | 131626 | 62.9 | 0.07 |
| MOPSO | 14 | 27 | 77 | 234 | 95.19 | 1.59 | 87877  | 137929 | 65.5 | 0.03 |
| MOPSO | 15 | 19 | 77 | 100 | 94.83 | 1.38 | 37688  | 63806  | 55.2 | 0.11 |

## References

- 1 S. T. Knox, S. J. Parkinson, C. Y. P. Wilding, R. A. Bourne and N. J. Warren, *Polym. Chem.*, 2022, **13**, 1576–1585.
- 2 E. Bradford, A. M. Schweidtmann and A. Lapkin, TS-EMO, <https://github.com/Eric-BRADFORD/TS-EMO>.
- 3 A. M. Schweidtmann, A. D. Clayton, N. Holmes, E. Bradford, R. A. Bourne and A. A. Lapkin, *Chem. Eng. J.*, 2018, **352**, 277–282.
- 4 Y. Tian, R. Cheng, X. Zhang and Y. Jin, *IEEE Comput. Intell. Mag.*, 2017, **12**, 73–87.
- 5 N. Islam and J. Oyekan, in *Conference on Genetic and Evolutionary Computation*, Lisbon, 2023.